Resolving cell state in iPSC-derived human neural samples with multiplexed fluorescence imaging

Martin L. Tomov, Alison O'Neil, Hamdah S. Abbasi, Beth Cimini, Anne Carpenter, Lee Rubin*, Mark Bathe*
Stanley Center for Psychiatric Research, Broad Institute of MIT and Harvard
Dept. of Stem Cell and Regenerative Biology, Harvard University
Dept. of Biological Engineering, MIT, Cambridge, MA

Correspondence to: Lee Rubin lee_rubin@harvard.edu and Mark Bathe mark.bathe@mit.edu

ABSTRACT

Human induced pluripotent stem cell-derived (iPSC) neural cultures offer clinically relevant models of human diseases, including Amyotrophic Lateral Sclerosis, Alzheimer's, and Autism Spectrum Disorder. In situ characterization of the spatial-temporal evolution of cell state in 2D and 3D culture models and organoids based on protein expression levels and localizations is essential to understanding neural cell differentiation, disease state phenotypes, and sample-to-sample variability. Here we apply PRobe-based Imaging for Sequential Multiplexing (PRISM) to facilitate multiplexed imaging with facile, rapid exchange of imaging probes to analyze iPSC-derived cortical and motor neuron cultures that are relevant to psychiatric and neurodegenerative disease models, using over ten protein targets. Our approach permits analysis of cell differentiation, cell composition, and functional marker expression in both standard 2D cultures and 3D spheroid and organoid sections. Further, our approach is amenable to automation, offering in principle ability to scale-up to dozens of protein targets and samples.

Introduction

Induced pluripotent stem cell (iPSC)-derived cultures are increasingly becoming the principal source of patient-specific and disease-specific cellular material for *in vitro* disease modeling. iPSC-derived cortical and motor neuron cultures have successfully been used to model neurodevelopmental conditions including autism spectrum disorder (ASD; cortical neurons) [1-5] and neurodegenerative conditions including spinal muscular atrophy and amyotrophic lateral sclerosis (SMA, ALS; motor neurons) [6-9]. Such iPSC-based models are attractive because they can generate the large numbers of neural cells needed for drug screening. They can also recapitulate aspects of cortical and motor neuronal synaptic networks, which allow for functional models of neurodevelopmental and neurodegenerative conditions to be developed *in vitro*. However, phenotypic characterization of these cultures is challenging due to their complexity, heterogeneity, and variability; this provides a clear opportunity for improved high content analysis techniques, especially those that can produce multidimensional readouts from the same culture.

Fluorescence-based antibody staining of target markers is one approach to characterizing in situ stem-cell derived neural cultures, but is limited by the conventional spectral limit of fluorophores to imaging four targets simultaneously. One technique to overcome this limitation uses DNA-conjugated antibodies to fluorescently image more than 10 individual markers in the same sample [10, 11]. This procedure, called PRobe-based Imaging for Sequential Multiplexing (PRISM), eliminates the need for antibody stripping or removal for multiplexing, a limiting factor in traditional immunofluorescence/immunocytochemistry (IF/ICC)-based multiplexed imaging strategies [12, 13], thereby allowing characterization using a greater number of molecular targets. Briefly, PRISM antibodies use short, orthogonal oligonucleotide sequences that are complementary to either a fluorophore-conjugated locked nucleic acid (LNA) or DNA strand that reversibly hybridizes to produce a fluorescent readout, analogous to traditional IF/ICC imaging [11, 14, 15] and DNA-PAINT/EXCHANGE-PAINT [14]. Further, compared to standard antibody stripping procedures [16-18], PRISM offers non-destructive imaging probe exchange, cycling fluorescent imaging strands within several minutes permitting multiple rounds of imaging data acquisition [19-21] from the same culture. These features allow the use of large panels of markers, consequently providing higher content datasets. Generation of oligo pairs is relatively straightforward due to the use of commercially available thiolated and fluorescently labelled oligo strands that can be readily conjugated to a wide variety of commercially available antibodies [11, 14, 15].

Here, we apply PRISM to 2D and 3D stem cell-derived cortical and motor neuron cultures to characterize cell identity and population composition based on detection of structural, synaptic, and transcription factor markers (**Figure 1**). Identification of multiple cell states within the same iPSC-derived 2D or 3D sample helps spatially map the temporal evolution and heterogeneity of targets in human samples, in addition to characterizing structural and synaptic features pertinent to human disease phenotypes [22-24]. We also introduce a CellProfiler/FIJI computational pipeline to analyze imaging data regarding cell state/phenotype in an automated, quantitative, unbiased manner [23, 24]. 2D cultures can be used for high-throughput characterization of stem cell-derived neurons, which lends itself well to automation assays, whereas 3D organoid sections retain the higher order structure of cellular organization, especially in neural cultures, which can be critical for disease modeling *in vitro*. Because PRISM is a direct analog to IF/ICC imaging, our approach complements assays in model culture systems currently used to evaluate stem cell differentiation, compound and drug candidate screening, tissue engineering, and potentially *in vitro* disease diagnostics development.

RESULTS

We built 12 antibodies into a PRISM panel to characterize the cellular composition of iPSC-derived CN and MN cultures. Specificity of target imaging was confirmed using traditional IF and compared to respective PRISM markers. We used established stem cell-derived astrocyte, CN, and MN cultures to screen a large panel of neural markers (**SI Table 1**)- before narrowing down to a panel of 12 PRISM-compatible antibodies (**SI Table 2**, **Figure 2a**). Based on staining intensity, signal specificity, and co-localizations between target markers, we were able to use 3+ specific markers to define a cell's identity (**SI Table 2 and Figure 2a**). For each selected antibody, we further compared the staining signal between IF/ICC and PRISM before and after PRISM conjugation (**Figure 2b and SI Figure 4**) to ensure each was still highly selective for its target and that the fluorescence pattern was consistent and unchanged between IF/ICC control and PRISM signal (**SI Figure 7**).

Newly generated DNA imaging strands were supplemented with published LNA imaging strands [11] for an initial round of 10 DNA-PRISM pairs (**SI Table 7** and **SI Figure 4** and **SI Figure 5**). Fluorescence signals were suitable for both manual and automated quantification of all 10 PRISM markers and 2 control IF/ICC markers (**SI Figure 6**). In order to confirm that PRISM signal is significantly above background, and thus suitable to imaging, we compared DNA-PRISM with traditional IF using cross-correlation analysis to map specific PRISM signals to subsequent IF signals in the same culture validated all 12 markers in human iPSC-derived CN (**SI Figure 7**) and in rat hippocampal neurons validated the tested markers (**SI Figure 8**). A full DNA-PRISM marker panel in rat hippocampal neurons was performed, showing that DNA-PRISM can be used to characterize neural cultures from different organisms while maintaining specificity of marker staining patterns (**SI Figure 9**).

Validation and optimization included matching staining patterns in primary rat hippocampal neurons and human stem cell-derived (BJ-SiPs) CN between control IF/ICC and PRISM by Pearson Correlation analysis with values ranging between 0.65 (synaptic markers) and 0.89 (cytoskeletal markers), and signal-to-noise ratios of at least 25:1 based on pixel intensity [A.U.], and minimal off-target binding and non-specific signal between the validated oligos and any present cell DNA or RNA transcripts, which is necessary for imaging nuclear transcription factors and to reduce non-specific binding to native DNA and/or RNA even after salmon sperm DNA blocking and RNAse treatment.

PRISM enables high content imaging of over ten neural markers in 2D and 3D iPSC-derived CN and MN cultures. 3D iPSC-derived CN and MN cultures were dissociated, plated in standard 2D culture wells, maintained for 14 days, and then fixed and stained for analysis. First, BJ-SiPs iPSCs were differentiated into CN (**SI Table 4**) and characterized via multiple markers by traditional IF/ICC to confirm their cortical nature (**SI Figure 1**). Representative images of the 2D CN culture illustrate multiple cell subtypes (**Figure 3a**). We further characterized in-depth two time points during differentiation of cortical cultures in relation to cell identity (**Figure 3b**). At day 55 of cortical differentiation, there were 84 cells that fulfilled our analysis criteria (**Figure 2a**) where we were able to positively identify 30% of the analyzed cells as neurons. Synaptic marker staining characterized 100% of identified neurons as excitatory in this earlier culture (VGLUT1+). Immature/inactive astrocytes (CD44+/Vimentin+) made up 18% of the culture and 7% of the cells expressed markers for mature/activated astrocytes (CD44+/GFAP+). We were also able to positively identify both neural progenitor cells (2%, Pax6+) and a significant percentage of radial glial cells (36%, Pax6+/Vimentin+). Cells that were present but could not be positively identified

represented 7% of the total population. We then followed up with a day 85 differentiation timepoint, where we identified 161 cells that fulfilled the criteria for analysis as outlined in the Methods section. Of these, 58% were positively identified as neurons (Tuj1+/MAP2+) and 26% as astrocytes (CD44+/Vimentin+/GFAP+). Neurons were successfully further sub-typed based on synaptic marker expression into either excitatory (52%, VGLUT1+) or inhibitory (3%, VGAT+). The remaining 45% of identified neurons were not strongly associated with either type. Astrocytes were further characterized as either immature/inactive (19%, Pax6-/Vimentin+/CD44-) or mature/active (7%, Pax6-/GFAP+/CD44+). We observed no significant presence of either neural progenitor (Pax6+) or radial glial cells (Pax6+/Vimentin+). We were unable to classify 16% of cells present, based on our characterization criteria.

A parallel PRISM assay of iPSC-derived 2D MN cultures validated the full panel of conjugated antibodies (**Figure 4**) to characterize the MN cultures in a similar manner. To validate that the generated neuronal cells are indeed motor neurons, we stained separate wells on the same plate with the motor neurons markers Islet 1 and 200kD neuroflament protein (**SI Figure 2**) Subsequently, PRISM antibodies generated highly specific signals, and the images were then overlaid to generate high-content imaging datasets. We show here that DNA-PRISM antibodies can characterize complex stem cell-derived cultures in a multi-dimensional manner with the added ability to preserve the spatial relationships between the markers used in our characterization pipeline. Further optimization to improve staining quality by testing antibodies that are generated to produce high specificity and optimized signal-to-noise ratios in the putative MN cultures in particular is ongoing.

Automated pipeline to pair PRISM high-content data analysis with high throughput data generation. Due to the high volume of raw data that is generated in a PRISM imaging assay, we endeavored to develop an automated platform that could manage staining, imaging, and data analysis in the same pipeline. We first identified key points in our manual PRISM assay data acquisition process, namely buffer exchanges, imager strand incubation, and IF/ICC imaging, and automated them using a BRAVO liquid handler and a PerkinElmer Phenix spinning disk confocal microscope. Next, points of adaptation within the physical assay steps such as buffer volume, aspiration and dispensing speed, and incubation times were streamlined to improve automation. Slowing buffer aspiration and addition into the wells significantly reduced cell detachment and damage during the twenty consecutive buffer exchanges that were necessary for a complete PRISM assay. Representative PRISM staining performed with automation (**SI Figure 10a)** was comparable to manual PRISM staining and imaging (**Figure 3a**). While the average time for data acquisition was similar between the manual and automated assays, incorporating automated CellProfiler and FIJI analysis pipelines (available upon request) reduced the analysis time by almost 3-fold resulting in an overall reduction of assay duration, while increasing throughput (**SI Figure 10b)**.

DISCUSSION

Recently, high content analysis has been used to characterize multiple neurological cell types and their interactions *in vivo* and *in vitro* [25, 26], providing insights into cell differentiation and neurological conditions [27-31]. Such work can benefit from a complementary IF method that is not constrained by limitations inherent in traditional antibody-based imaging. In our analysis, we used DNA- and LNA-conjugated PRISM antibodies to evaluate complex CN and MN cultures derived from stem cell lines in both 2D cultures and in 3D organoid sections (data not shown). In future studies, we envision that PRISM may be used for large scale analysis of neural disease initiation and progression, such as in ALS, focusing on morphology, synaptic make-up and interactions between neurons and glial cells that are present in these cultures [32].

We used PRISM to perform multi-dimensional characterization of heterogeneous cell types that have direct pharmacological and disease modeling applications. DNA/DNA or DNA/LNA pair strands with a number of fluorophore modifications are readily available from commercial vendors, making such antibody panels relatively straightforward to generate for a wide range of research applications. Wang et al. [33] reported that DNA-only oligos can have significant non-specific binding to native transcripts. To mitigate this issue, we implemented a salmon sperm DNA blocking step, as well as RNAse pre-treatment of the fixed cultures when LNA strands were used (see **SI Table 3** for detailed protocol). We further chose DNA oligo pairs between 11-12 nucleotides with GC content between 30-40%, which we found to be optimal for reducing background fluorescence while still allowing complete washout or exchange of imaging strands post-acquisition. High melting temperature of the DNA/LNA oligos may push PRISM into a range where samples need to be heated, even under low salt concentration, in order to release imaging strands. High melting temperature also can cause fluorescence artifacts such as residual signal and non-specific binding and increased cell detachment due to the need for heating and cooling of the sample, thereby complicating assay automation [21, 34, 35]. While fluorescence from the PRISM staining was considerably lower than the corresponding signal from conventional secondary antibodies (**SI Figure 4c**), it was still well above backround levels and this potential limitation coul be overcome with further development of the technique to increase number of fluorophores on the imager strands, or with longer exposure times.

The 12 markers that we used in our assay allowed in depth analysis suggesting that disease-specific morphological and gene expression differences could be elucidated. These findings open the door to using PRISM antibodies for drug screening and characterizing *in vitro* disease models. We further expanded our fluorophore detection lines from one [11] to two, halving the time necessary for imaging and reducing the number of wash steps, which decreased cell detachment, thus improving our multi-dimensional analysis reproducibility. To take full advantage of the multi-dimensional data set that was generated, we incorporated in-depth analysis capabilities using a custom CellProfiler pipeline. This pipeline can characterize cell subsets within cultures in general, and in the cortical cultures, characterize the localization and density of synaptic markers within defined neurites. PRISM would likely be especially well suited to support studies of polygenic psychiatric conditions (Autism Spectrum Disorder and Schizophrenia), neurodevelopmental (ALS), and neurodegenerative (Parkinson's and Alzheimer's) conditions, which are characterized by multiple contributing genes and protein targets [36-42].

MATERIALS AND METHODS

Consent for use of human material. All human material (iPSC lines) was obtained with informed consent and used with the approval of the Harvard University IRB and ESCRO committees. The BJ-SiPs cell line was derived from a healthy male donor using Sendai virus reprogramming. The 39B stem cell line was derived from a female donor that was positive for Amyotrophic lateral sclerosis (SOD1A4V), using retroviral integration of the transgenes Oct4, Sox2, KLF4. The 1016A stem cell line was derived from a healthy male donor using Sendai virus reprogramming.

DNA-PRISM antibody marker selection, conjugation, and validation. Starting from a list of commonly used neural culture-specific antibodies (**SI Table 1**), we chose a set of twelve markers to build the PRISM antibody panel (**Figure 2**). The antibody panel features housekeeping and structural targets (α-Tubulin, Actin), markers for canonical neural culture characterization (Tuj1, Map2, Synapsin I, GFAP, Vimentin, CD44), as well as cell-specific markers, including those for identifying cortical (VGAT, VGLUT1) and motor neurons (Islet1), glial cell subtypes (Vimentin, GFAP, CD44), neural progenitor cells (Pax6), and residual pluripotent cells (Oct4A) that might have been retained post-differentiation (**SI Table 2)**. For each antibody, validation was first performed using standard IF/ICC prior to oligo conjugation.

Confocal imaging of control markers and PRISM panel. Cultures were fixed in 4% paraformaldehyde for 15 min at room temperature, then washed in phosphate buffered saline (PBS) and stored at 4°C until they were stained and imaged. Immediately prior to staining, fixed cultures were quenched in 100 mM glycine in ddH_2O for 10 min at room temperature. After quenching, the fixed cells were permeabilized in 0.2% Triton X-100 in PBS for 15 min at room temperature and blocked in 2% bovine serum albumin (BSA) in PBS supplemented with 1 mg/ml salmon sperm DNA (catalog #D7656; Sigma-Aldrich) for 1 hour at 4°C. For marker validation and optimization of staining conditions, cultures were imaged on a Nikon Ti-E spinning disk confocal microscope. High-content imaging with the validated conjugated antibodies panel was then carried out on a PerkinElmer Opera Phenix high-content confocal microscope. The PRISM imaging sequence was performed as previously described [11], with the following modifications. We used all primary antibodies in the panel, both in regular IF/ICC and for PRISM assays, at 1:400 dilution and all secondary fluorophore-conjugated antibodies at 1:1000 dilution for IF. Secondary PRISM-conjugated antibodies were used at 1:200 dilution. We used highly cross-adsorbed secondary antibodies raised in donkey for PRISM, to minimize any possible signal cross-talk and fluorophore conjugated secondary antibodies also raised in donkey as negative/positive controls. The full list of antibodies is provided in **SI Table 1**, with specific staining protocols for DNA-PRISM, including imaging/other buffers, provided in **SI Table 3**.

Induced pluripotent stem cells (iPSCs) maintenance. Human iPSCs (BJ-SiPs, 1016A, and 39B) were maintained feeder-free on Matrigel hESC-Qualified Matrix (catalog #354277; Corning) coated plates in StemFlex (catalog #A3349401; ThermoFisher) or mTeSR1 (catalog #85857; STEMCELL Technologies) medium to maintain pluripotency and for expansion. Both media were supplemented with pen/strep (1x; catalog #15140122; Gibco). Media were changed every other day for StemFlex and every day for mTeSR1, with cells passaged when they reached >80% confluence.

Neural progenitor cells (NPCs) maintenance. Human NPCs were generated using the STEMdiff SMADi neural induction kit (catalog #08581; STEMCELL Technologies) according to the

manufacturer's instructions. Briefly, dissociated iPCSs were seeded as a monolayer on Matrigel-coated plates in the provided neural induction medium (NIM) for 14 days, with daily medium changes. NPC expansion, where needed, was performed in Neural Progenitor Medium (catalog #05833; STEMCELL Technologies) from the same kit. On average, NPCs doubled every 3-5 days.

Rat primary hippocampal neurons maintenance. Dissociated rat hippocampal neurons were plated on Matrigel-coated plates and maintained in Neurobasal (NB) Medium (catalog # 21103049 ThermoFisher) supplemented with B27 with insulin (1x; catalog #17504044 Gibco), non-essential amino acids (1x catalog #11140050 Gibco) and 1x pen/strep for 21 days, with half medium changes every 5 days.

Human iPSC-derived cortical neuron differentiation and maintenance. Human cortical neurons (CN) were differentiated as spheroids in a 3D spinner flask based on previously established protocols [43, 44] with some modifications. Pluripotent iPSCs were dissociated into single cell suspensions using Accutase (1x; catalog #07920 STEMCELL Technologies) for 10 minutes at 37^{o}C. Cells were then adapted to a spinner flask at a concentration of 1x10^{6} cells/mL in mTeSR1 medium supplemented with rho kinase (ROCK) inhibitor, Y-27632 (10 μM; catalog #SCM075 EMD Millipore) for 2 days. Neural progenitor patterning with the small molecules SB431542 (10 μM; catalog #1614 Tocris), LDN193189 (1 μM; catalog #6053 Tocris) and XAV939 (2 μM; catalog #3748 Tocris) was carried out over the next 4 days, with full medium changes every day. Cells were grown in mTeSR1 supplemented with the above factors for the initial 24 hours, then the cells were maintained in Knockout Serum Replacement (15% KSR; Thermo Fisher Scientific) medium for the next 3 days, again supplemented with the above factors. Between days 5 to 11, we gradually transitioned the cells into NIM as follows. On day 5, 75% KSR Pulse medium was mixed with 25% NIM medium supplemented with SB431542 (10 μM) and LDN193189 (1 μM) and cells were incubated for 2 days. On day 7, 50% KSR medium and 50% NIM medium were supplemented with LDN193189 (1 μM) for another 2 days. On day 9, cells were kept in 25% KSR mixed with 75% NIM medium with LDN193189 (1 μM) for another 2 days. On day 11, the 3D cultures were fully transitioned to NIM medium for 9 days with full medium changes every 3 days. The NIM medium at this point was not supplemented with any additional small molecules. On day 20, spheroids were transitioned to NB medium, supplemented with B27 Supplement (1x; catalog #A3582801 ThermoFisher), N2 Supplement (1x; catalog #17502048 ThermoFisher), brain-derived neurotrophic factor (BDNF; 10 ng/mL; catalog #248-BD-010 Tocris) and glial cell-derived neurotrophic factor (GDNF; 10 ng/mL; catalog #212-GD-010 Tocris) and maintained with full medium changes every 4 days until day 40. At this point, mitotically active cortical progenitors could be cryo-stored or maintained as spheroids for a further 14 days or more (up to 100 days) to generate mature CN for functional analysis, with 50% medium changes every 3 days. For staining and analysis, spheroids were dissociated in 0.25% Trypsin-EDTA (catalog #15575020 Thermofisher) to single cells. The cell suspension was plated into 96-well plates that were previously coated with poly-D-lysine (25 μg/mL) and poly-L-ornithine (25 μg/mL) overnight at 37°C, and then further coated with Laminin ((10 μg/mL; catalog #11243217001 Sigma-Aldrich) for 3 hours at 37°C. These 2D cultures were then matured for an additional 14 days prior to DNA-PRISM marker analysis, with 50% medium changes every 3 days. See **SI Table 4** for detailed protocol steps and **SI Figure 1** for representative images of cortical cultures

Human iPSC-derived motor neuron differentiation and maintenance. Motor neurons (MN) were generated using a modified version of previously established protocols [45, 46]. iPSC colonies were dissociated into single cells using Accutase. Cells were then seeded into ultra-low

attachment dishes in mTESR1 medium supplemented with ROCK inhibitor, Y-27632 (10 μM; catalog #1254 Tocris) and basic fibroblast growth factor (FGF-2; 20 ng/mL; catalog #233-FB-010 Tocris) for the first 24 hours to allow for embryoid body (EB) formation. The following day, ROCK inhibitor was removed, and fresh mTESR1 was added to the cultures. Forty-eight hours after EB aggregation, cells were switched to MN Differentiation Medium: Advanced DMEM/F-12 (catalog #12634010 ThermoFisher) & NB Medium (50:50 v/v), 1x N-2 supplement, 1x B27+Insulin, 1x GlutaMAX (catalog #A1286001 ThermoFisher), 1x pen/strep, and 0.1 mM 2-mercaptoethanol (catalog #31350010 ThermoFisher). To specify neural patterning, dual SMAD inhibition was used with small molecules SB431542 (10 μM) and LDN193189 (100 nM) from day 0 to day 6 of differentiation. From day 0 to day 4 the glycogen synthase kinase 3 inhibitor, CHIR99021 (3 μM; catalog #4423 Tocris) was added to increase the population of Olig2 positive MN progenitors. Beginning on day 2, MN specification was induced with 1 μM All-trans Retinoic Acid (at-RA; catalog #0695 Tocris) and 1 μM Smoothened Agonist (SAG; catalog #4366 Tocris; assuming that's what you used) until day 16. The y-secretase inhibitor, (2S)-N-[(3,5-Difluorophenyl)acetyl]-L-alanyl-2-phenyl]glycine 1,1-dimethylethyl ester (DAPT, catalog #2634 Tocris) was used at 10 μM in conjunction with neurotrophic factors BDNF and GDNF (10 ng/mL each) starting on day 8 until day 16 of differentiation, with 50% medium changes every 2 days. Spheroids were then dissociated with a solution containing 0.25% Trypsin-EDTA and DNAse (25 μg/mL; catalog #18047019 ThermoFisher), and plated onto poly-L-ornithine (25 μg/mL; catalog #P2533-10MG Sigma-Aldrich), Fibronectin (10 μg/mL; catalog #11051407001 Sigma-Aldrich), and Laminin (10 μg/mL)- coated plates in medium supplemented with BDNF and GDNF (10 ng/mL each). See **SI Table 5** for detailed protocol steps and refer to **SI Figure 2** for differentiation protocol outline and representative images of MN cultures.

Human iPSC-derived astrocyte differentiation and maintenance. Human NPCs were expanded as progenitors and then seeded at ~20% confluence onto Matrigel-coated tissue culture plates. Commercial astrocyte medium (catalog #1801 Sciencell) was used to differentiate NPCs as previously described [47, 48]. Briefly, starting with ~40% confluent NPC cultures, astrocyte medium was changed every 3-4 days and cells were passaged at 1:10 ratio when they reached ~80-90% confluence for the first 28 days. Immature astrocytes generated by this method express multiple canonical glial markers and were further matured via small molecules or exposure to FBS/Matrigel into GFAP+ cells [49]. See **SI Figure 3** and **SI Table 6** for detailed protocol and representative images.

Design of imaging strands for PRISM antibody conjugation. We designed new DNA imaging strands and used previously published LNA sequences to generate stable PRISM pairs by varying their length and altering the GC content of the oligos (**SI Table 7**).

Automated pipeline for antibody staining, imaging, and characterization of cortical cultures. To validate PRISM antibodies for automation suitability, we performed IF imaging on two high content plate confocal microscopes, the PerkinElmer Opera Phenix and the Molecular Devices ImageXpress. Once antibody signal was confirmed, IF staining of cortical cultures (**SI Figure 10**) was adapted to 96-well plates and was partially automated using a BRAVO liquid handler (Agilent); dispensing 100 µl of either buffer, antibody, or PRISM reagent per well (See **SI Table 3** for details on buffer compositions and dilutions). The system was programmed to perform an initial rinse with Wash Buffer, then each well was aspirated and 100 µl of fresh Imaging Buffer with PRISM imaging strands was added and incubated at room temperature for 10 min. Plates were then rinsed three times with Imaging Buffer and imaged on a PerkinElmer Opera Phenix at 20X, with the 405 nm

laser for Hoechst nuclear stain (IF), 488 nm laser for Actin (IF), and 590 nm and 647 nm lasers for PRISM antibodies. Exposures were either 300 ms (PRISM antibodies) or 150 ms (ICC controls). Post-imaging, each well was washed three times with Wash Buffer and incubated for 5 min between washes to eliminate residual PRISM imaging strand signal. Control imaging was performed after the third rinse to confirm removal of imaging strands prior to subsequent imaging strand addition and imaging rounds. These steps were repeated until all PRISM antibodies in the panel were imaged. Further automation was achieved by incorporating robotics to move the plates for confocal imaging to the PerkinElmer Opera Phenix high content platform at 60X magnification, where each well was imaged in a 4x4 tile pattern, covering roughly 10% of the well area. Based on cell type-specific markers that have been validated in the field (**SI Table 2**), we then built up a querry algorithm to identify each cell subtype we were interested in within the differentiated cultures. Only cells that were positive for all the required markers were included in the analysis groups within each sub-type. A detailed breakdown on cellular characterization is shown in **Figure 2a**.

Data were analyzed using custom CellProfiler (cellprofiler.org) and FIJI (https://fiji.sc/) pipelines for post-processing and image analysis of high-content PRISM data (reference code is available upon request). Each image from the PRISM assay was aligned in sequential imaging rounds using the nuclear (Hoechst 33342; 405 nm) and actin (Phalloidin; 488 nm) channels. The aligned signal from each marker was then overlaid in a composite image that was then analyzed for protein co-localization within the cells, expression patterns of specific markers in the culture and levels of protein expression. Only cells that were present in all image sequences of an experiment, based on the overlays, were fed to the CellProfiler analysis pipeline to characterize the neural cultures. Sampling data from 12 markers, i.e., 5 probe addition/imaging sequences, allowed us to generate multi-stain identity of cellular populations that were designated as neurons (cortical or motor), astrocytes, neural stem cells, etc., building cellular composition profiles of the tested iPSC-derived cortical and motor neuron cultures.

DATA AVAILABILITY

The data that support the findings of this study are available from the corresponding author upon reasonable request.

References

1. Andoh-Noda, T., et al., *Modeling Rett Syndrome Using Human Induced Pluripotent Stem Cells.* CNS Neurol Disord Drug Targets, 2016. **15**(5): p. 544-50.
2. Avior, Y., I. Sagi, and N. Benvenisty, *Pluripotent stem cells in disease modelling and drug discovery.* Nat Rev Mol Cell Biol, 2016. **17**(3): p. 170-82.
3. Bourgeron, T., *From the genetic architecture to synaptic plasticity in autism spectrum disorder.* Nat Rev Neurosci, 2015. **16**(9): p. 551-63.
4. Marchetto, M.C., et al., *A model for neural development and treatment of Rett syndrome using human induced pluripotent stem cells.* Cell, 2010. **143**(4): p. 527-39.
5. Ooi, L., et al., *Induced pluripotent stem cells as tools for disease modelling and drug discovery in Alzheimer's disease.* J Neural Transm (Vienna), 2013. **120**(1): p. 103-11.
6. Barral, S. and M.A. Kurian, *Utility of Induced Pluripotent Stem Cells for the Study and Treatment of Genetic Diseases: Focus on Childhood Neurological Disorders.* Front Mol Neurosci, 2016. **9**: p. 78.
7. Di Giorgio, F.P., et al., *Human embryonic stem cell-derived motor neurons are sensitive to the toxic effect of glial cells carrying an ALS-causing mutation.* Cell Stem Cell, 2008. **3**(6): p. 637-48.
8. Di Giorgio, F.P., et al., *Non-cell autonomous effect of glia on motor neurons in an embryonic stem cell-based ALS model.* Nat Neurosci, 2007. **10**(5): p. 608-14.
9. Lindvall, O. and Z. Kokaia, *Stem cells for the treatment of neurological disorders.* Nature, 2006. **441**(7097): p. 1094-6.
10. Kulikov, V., et al., *DoGNet: A deep architecture for synapse detection in multiplexed fluorescence images.* PLoS Comput Biol, 2019. **15**(5): p. e1007012.
11. Guo, S.M., et al., *Multiplexed and high-throughput neuronal fluorescence imaging with diffusible probes.* Nat Commun, 2019. **10**(1): p. 4377.
12. Micheva, K.D. and S.J. Smith, *Array tomography: a new tool for imaging the molecular architecture and ultrastructure of neural circuits.* Neuron, 2007. **55**(1): p. 25-36.
13. Micheva, K.D., et al., *Array tomography: high-resolution three-dimensional immunofluorescence.* Cold Spring Harb Protoc, 2010. **2010**(11): p. pdb top89.
14. Jungmann, R., et al., *Multiplexed 3D cellular super-resolution imaging with DNA-PAINT and Exchange-PAINT.* Nat Methods, 2014. **11**(3): p. 313-8.
15. Xu, Q., et al., *Design of 240,000 orthogonal 25mer DNA barcode probes.* Proc Natl Acad Sci U S A, 2009. **106**(7): p. 2289-94.
16. Buchwalow, I.B., E.A. Minin, and W. Boecker, *A multicolor fluorescence immunostaining technique for simultaneous antigen targeting.* Acta Histochem, 2005. **107**(2): p. 143-8.
17. Lan, H.Y., et al., *A novel, simple, reliable, and sensitive method for multiple immunoenzyme staining: use of microwave oven heating to block antibody crossreactivity and retrieve antigens.* J Histochem Cytochem, 1995. **43**(1): p. 97-102.
18. Lewis Carl, S.A., I. Gillete-Ferguson, and D.G. Ferguson, *An indirect immunofluorescence procedure for staining the same cryosection with two mouse monoclonal primary antibodies.* J Histochem Cytochem, 1993. **41**(8): p. 1273-8.
19. Nieves, D.J., K. Gaus, and M.A.B. Baker, *DNA-Based Super-Resolution Microscopy: DNA-PAINT.* Genes (Basel), 2018. **9**(12).
20. Schnitzbauer, J., et al., *Super-resolution microscopy with DNA-PAINT.* Nat Protoc, 2017. **12**(6): p. 1198-1228.
21. Schueder, F., et al., *Multiplexed 3D super-resolution imaging of whole cells using spinning disk confocal microscopy and DNA-PAINT.* Nat Commun, 2017. **8**(1): p. 2090.
22. Zanella, F., J.B. Lorens, and W. Link, *High content screening: seeing is believing.* Trends Biotechnol, 2010. **28**(5): p. 237-45.

23. Schindelin, J., et al., *Fiji: an open-source platform for biological-image analysis.* Nat Methods, 2012. **9**(7): p. 676-82.
24. Carpenter, A.E., et al., *CellProfiler: image analysis software for identifying and quantifying cell phenotypes.* Genome Biol, 2006. **7**(10): p. R100.
25. Genovese, G., et al., *Increased burden of ultra-rare protein-altering variants among 4,877 individuals with schizophrenia.* Nat Neurosci, 2016. **19**(11): p. 1433-1441.
26. Ripke, S., et al., *Genome-wide association analysis identifies 13 new risk loci for schizophrenia.* Nat Genet, 2013. **45**(10): p. 1150-9.
27. Gulsuner, S., et al., *Spatial and temporal mapping of de novo mutations in schizophrenia to a fetal prefrontal cortical network.* Cell, 2013. **154**(3): p. 518-29.
28. van Rheenen, W., et al., *Genome-wide association analyses identify new risk variants and the genetic architecture of amyotrophic lateral sclerosis.* Nat Genet, 2016. **48**(9): p. 1043-8.
29. McLaughlin, R.L., et al., *Genetic correlation between amyotrophic lateral sclerosis and schizophrenia.* Nat Commun, 2017. **8**: p. 14774.
30. Tiziano, F.D., J. Melki, and L.R. Simard, *Solving the puzzle of spinal muscular atrophy: what are the missing pieces?* Am J Med Genet A, 2013. **161A**(11): p. 2836-45.
31. Yang, C.W., et al., *An Integrative Transcriptomic Analysis for Identifying Novel Target Genes Corresponding to Severity Spectrum in Spinal Muscular Atrophy.* PLoS One, 2016. **11**(6): p. e0157426.
32. Lindsay, M.A., *Target discovery*. Nat Rev Drug Discov, 2003. **2**(10): p. 831-8.
33. Wang, L., et al., *Locked nucleic acid molecular beacons.* J Am Chem Soc, 2005. **127**(45): p. 15664-5.
34. Agasti, S.S., et al., *DNA-barcoded labeling probes for highly multiplexed Exchange-PAINT imaging.* Chem Sci, 2017. **8**(4): p. 3080-3091.
35. Wade, O.K., et al., *124-Color Super-resolution Imaging by Engineering DNA-PAINT Blinking Kinetics.* Nano Lett, 2019. **19**(4): p. 2641-2646.
36. Betancur, C., *Etiological heterogeneity in autism spectrum disorders: more than 100 genetic and genomic disorders and still counting.* Brain Res, 2011. **1380**: p. 42-77.
37. Walsh, T., et al., *Rare structural variants disrupt multiple genes in neurodevelopmental pathways in schizophrenia.* Science, 2008. **320**(5875): p. 539-43.
38. International Schizophrenia, C., et al., *Common polygenic variation contributes to risk of schizophrenia and bipolar disorder.* Nature, 2009. **460**(7256): p. 748-52.
39. Shi, J., et al., *Common variants on chromosome 6p22.1 are associated with schizophrenia.* Nature, 2009. **460**(7256): p. 753-7.
40. Fromer, M., et al., *De novo mutations in schizophrenia implicate synaptic networks.* Nature, 2014. **506**(7487): p. 179-84.
41. Schizophrenia Working Group of the Psychiatric Genomics, C., *Biological insights from 108 schizophrenia-associated genetic loci.* Nature, 2014. **511**(7510): p. 421-7.
42. Dale, J.M., et al., *The spinal muscular atrophy mouse model, SMADelta7, displays altered axonal transport without global neurofilament alterations.* Acta Neuropathol, 2011. **122**(3): p. 331-41.
43. Rigamonti, A., et al., *Large-Scale Production of Mature Neurons from Human Pluripotent Stem Cells in a Three-Dimensional Suspension Culture System.* Stem Cell Reports, 2016. **6**(6): p. 993-1008.
44. Lancaster, M.A. and J.A. Knoblich, *Generation of cerebral organoids from human pluripotent stem cells.* Nat Protoc, 2014. **9**(10): p. 2329-40.
45. Maury, Y., et al., *Combinatorial analysis of developmental cues efficiently converts human pluripotent stem cells into multiple neuronal subtypes.* Nat Biotechnol, 2015. **33**(1): p. 89-96.

46. Du, Z.W., et al., *Generation and expansion of highly pure motor neuron progenitors from human pluripotent stem cells.* Nat Commun, 2015. **6**: p. 6626.
47. Pasca, A.M., et al., *Functional cortical neurons and astrocytes from human pluripotent stem cells in 3D culture.* Nat Methods, 2015. **12**(7): p. 671-8.
48. Tomov, M.L., et al., *Distinct and Shared Determinants of Cardiomyocyte Contractility in Multi-Lineage Competent Ethnically Diverse Human iPSCs.* Sci Rep, 2016. **6**: p. 37637.
49. So, P.T., et al., *Two-photon excitation fluorescence microscopy.* Annu Rev Biomed Eng, 2000. **2**: p. 399-429.

Manuscript Figures:

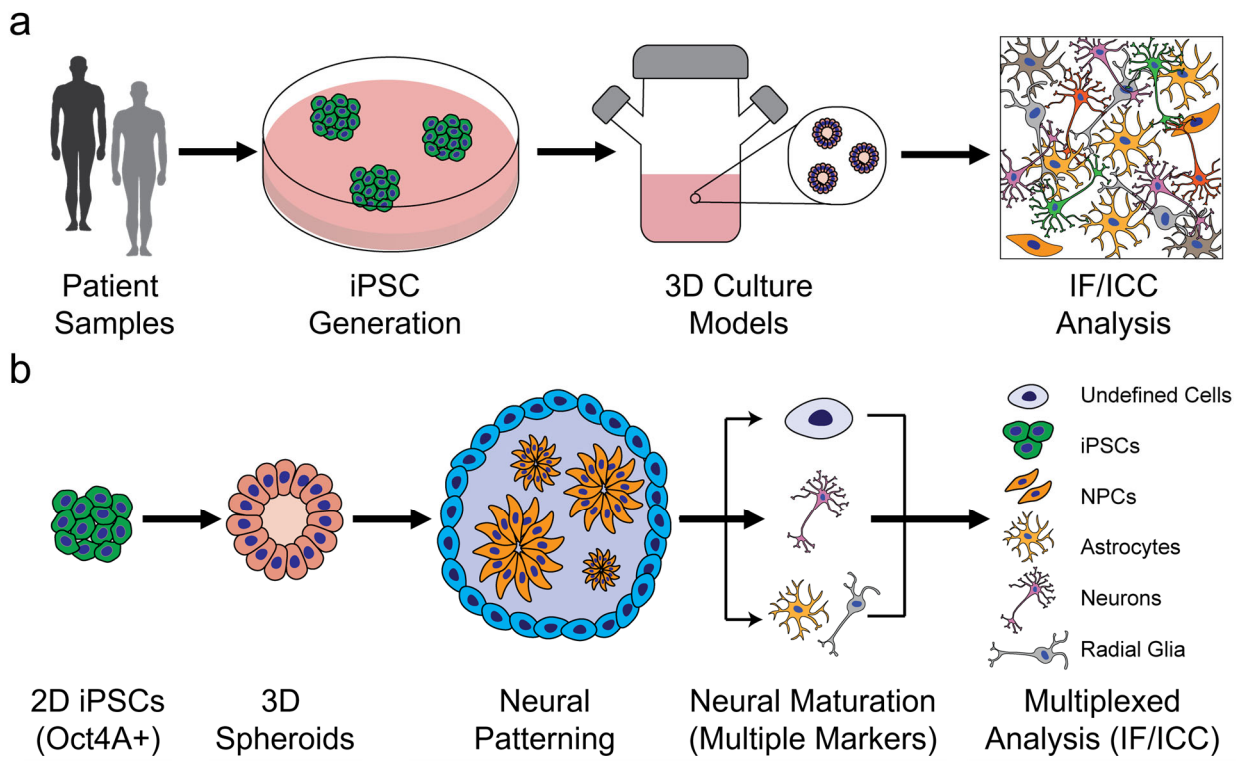

Figure 1: Generating stem cell derived disease models and complex neuronal cultures based on patient IPSCs requires careful and extensive validation. (a) Process flow to generate disease-specific stem cell lines from patients to model *in vitro* complex neurodevelopmental and neurodegenerative diseases using 3D spheroid cultures of cortical and motor neurons. **(b)** Stem cell-derived 3D neural cultures used to generate high-content data for culture and disease modeling. Cells are subsequently analyzed to generate specific culture breakdowns using PRISM for in-depth characterization of neural cultures via multiplexed staining.

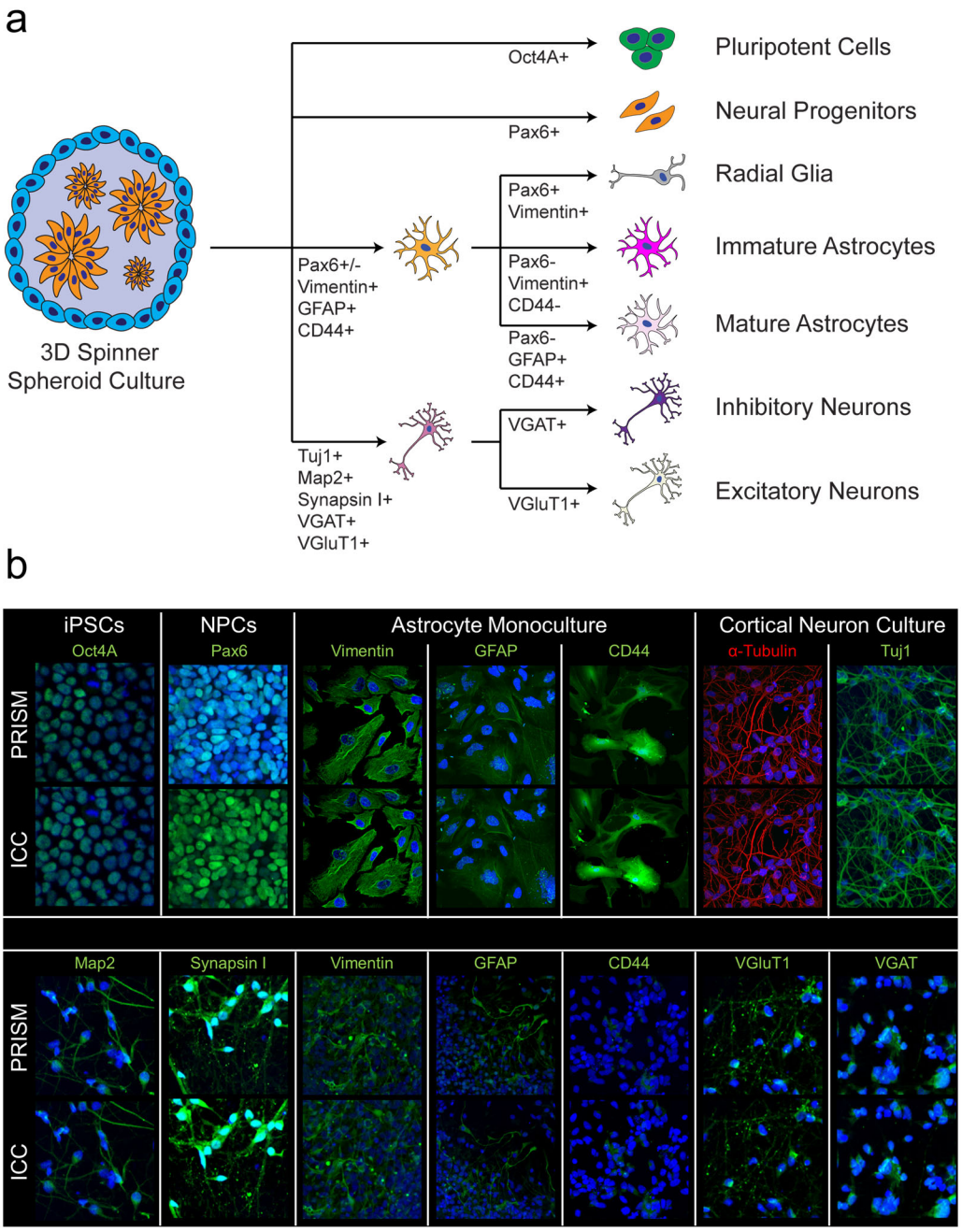

Figure 2: Breakdown of cell populations present in iPSC-derived neural cultures and validation staining of marker panel targets used in the in-depth characterization. A schematic **(a)** of the different cell types in a typical cortical culture that can be tracked via PRISM. The flow chart illustrates a representative readout of the breakdown of cell populations in cortical cultures. **(b)** ICC versus PRISM images of the markers used to characterize neural cultures. The Oct4A marker was imaged in the undifferentiated pluripotent state cell culture (iPCS), and the PAX6 marker was imaged in day 14 neural progenitor state cell culture (NPCs) for validation purposes.

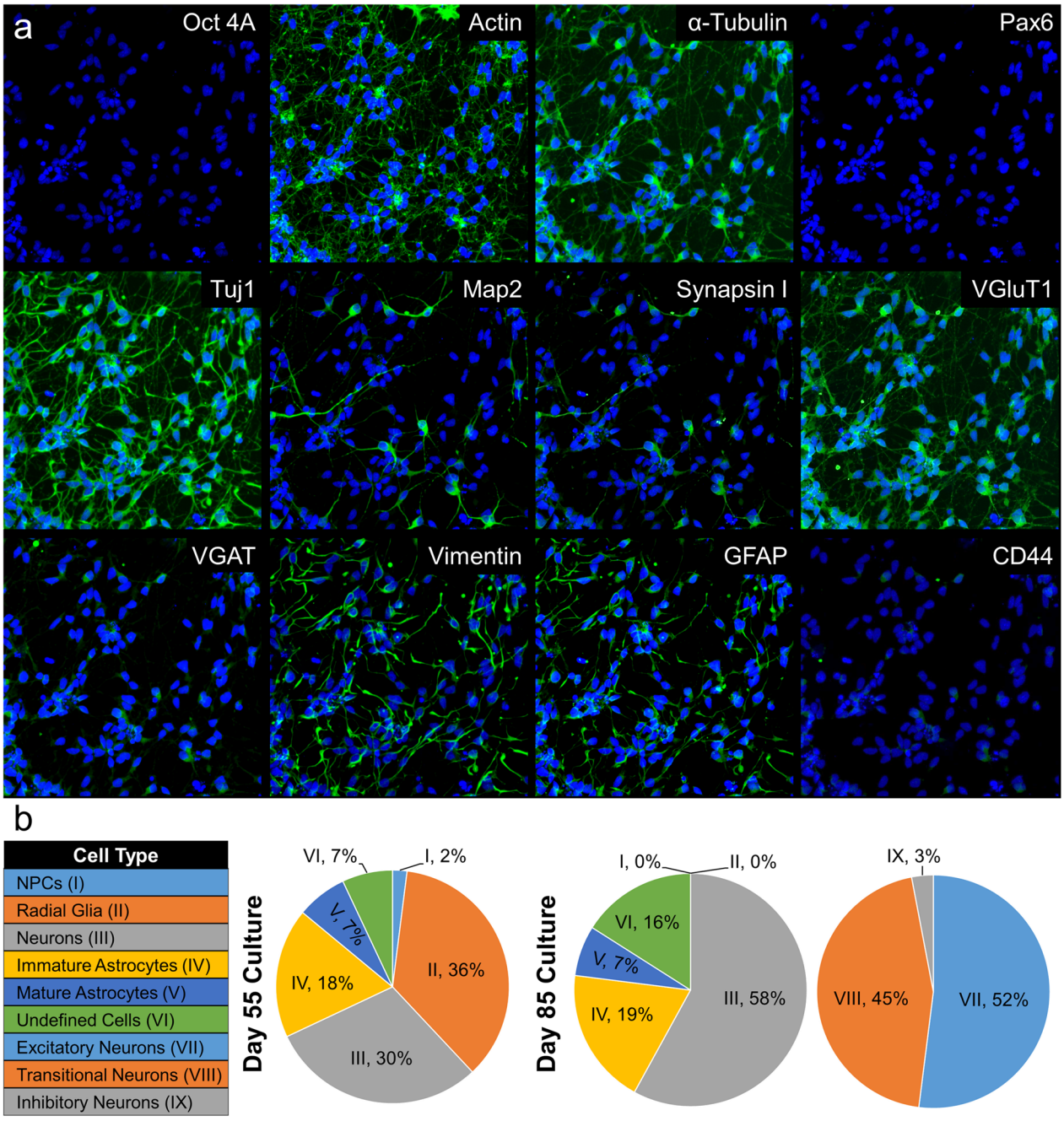

Figure 3: High-content analysis of dissociated cultures from hiPSC-derived cortical neurons. (a) Representative images from the same area of a 71 days old BJ-SiPs-derived cortical neuron culture, stained with the optimized 12-marker PRISM antibody panel, 14 days post-dissociation into 2D cultures. **(b)** CellProfiler quantification of cell types at 55 and 85 days in culture respectively.

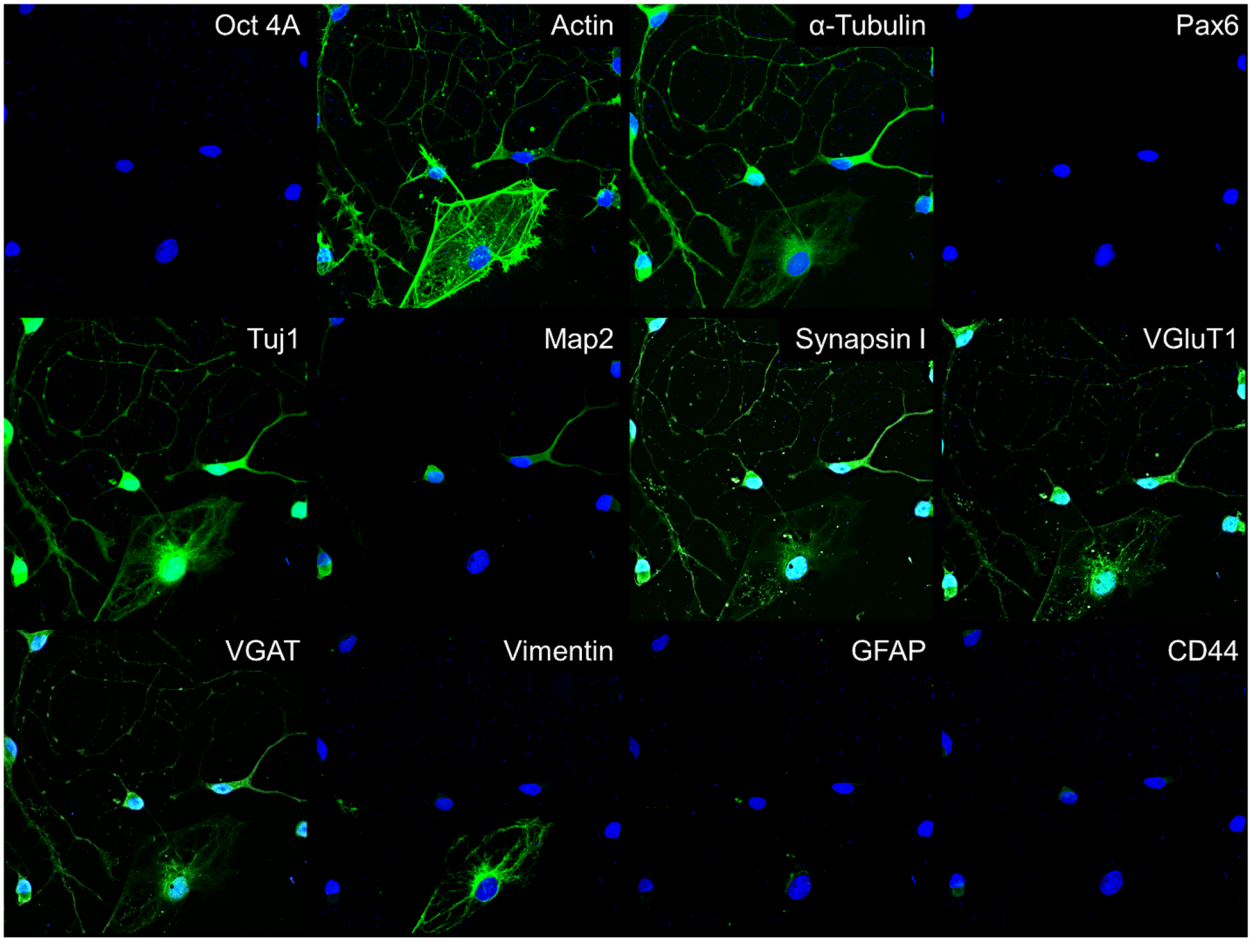

Figure 4: High-content IF/ICC analysis of dissociated cultures from hiPSC-derived motor neuron culture. Representative images from the same area of a 1016A-derived motor neuron culture, stained with the optimized 12-marker PRISM antibody panel after being grown for 21 days as a 3D spheroid, then dissociated into 2D and maintained for 14 days.